Reprogramming of MDSCs by ST316, a Clinical Peptide Antagonist of β-catenin/BCL9, Enhances Anti-tumor Immuno- and Chemotherapy

Claudio Scuoppo, Julia Diehl, Ricardo Ramirez, Barry J. Kappel, Abi Vainstein-Haras and Jim A. Rotolo. [1]Sapience Therapeutics, 520 White Plains Rd 2nd Floor, Tarrytown NY 10591

SAPIENCE THERAPEUTICS

Poster #3275

Introduction

Myeloid-derived suppressor cells (MDSCs) are a diverse group of immune cells that play critical roles in mediating immune-suppression. They are often associated with poor responses in various cancer types and represent an attractive target for immunotherapy. Challenges in defining the genetic dependencies of MDSCs have hindered development of effective therapeutic strategies aimed at targeting them.

The Wnt/β-catenin signaling pathway is a key oncogenic driver that has been implicated in immune-exclusion, although additional roles in immune-suppression remain unclear. ST316 is a clinical-stage peptide antagonist of the interaction between β-catenin and its co-activators, BCL9 and BCL9L. Currently, ST316 is being evaluated in a Phase 2 study (NCT05848739) in patients with advanced colorectal cancer (CRC) in combination with standard-of-care agents.

We demonstrated in a Phase 1 dose escalation study that ST316 suppresses MDSC expansion in the peripheral blood of treated patients and corroborated these findings in non-clinical CRC murine models. Here, we characterize the role of the Wnt/β-catenin/BCL9 pathway in MDSC programming and investigate the mechanism by which ST316 reduces MDSC expression and immuno-suppressive activity.

Transcriptional profiling of MDSCs from tumor-bearing mice indicates that β-catenin and other Wnt pathway components are highly expressed in these cells. Our findings indicate that exposure to ST316 reduces the expression of receptor systems linked to MDSC-mediated T-cell suppression, thereby activating T-cell responses in vivo. In combination studies, ST316 significantly enhances the anti-tumor efficacy of anti-PD-1 immunotherapy and standard-of-care chemotherapies for advanced CRC such as FOLFIRI. Moreover, while anti-PD-1 and FOLFIRI alone each resulted in expansion of immunosuppressive MDSCs, combination with ST316 prevented this expansion. Our results reveal a novel role for Wnt/β-catenin signaling in MDSC biology and demonstrate that ST316 can suppress the increase of therapy-driven MDSCs in vivo. These data suggest that therapeutically targeting the BCL9/β-catenin interaction may be an effective strategy to enhance both chemotherapy and immunotherapy in Wnt-driven tumors that respond poorly to monotherapy.

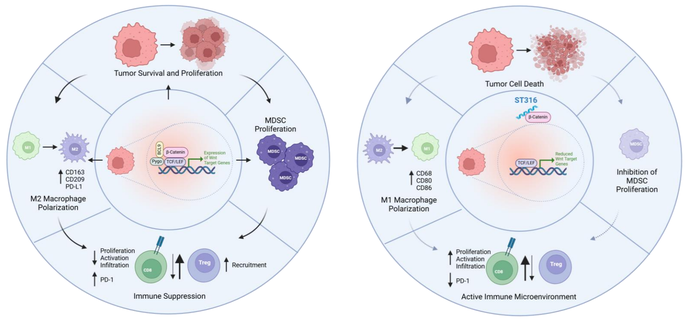

Figure 1. The Wnt/β-catenin pathway is a master regulator of both oncogenesis and immune evasion in the TME. (Top) In cancer cells, interaction of β-catenin with its co-activator BCL9 results in hyperactivation of a genetic signature that supports tumor cell survival and proliferation. Further, factors from Wnt/β-catenin-driven tumors promote immunosuppression by driving M2 polarization of TAMs and accumulation of immunosuppressive MDSC populations. (Bottom) ST316 antagonism of the interaction of β-catenin and BCL9 results in tumor cell death. Additionally, programs within the M2 TAMs and PMN-MDSC require Wnt/β-catenin, as disruption of β-catenin results in depletion of these cell populations. Collectively, depletion of immunosuppressive TAMs and MDSC populations drives a decrease in tumor infiltration of immunosuppressive T-regs and increased cytotoxic CD8 T cells, resulting in reversal of Wnt-driven immune exclusion.

Results

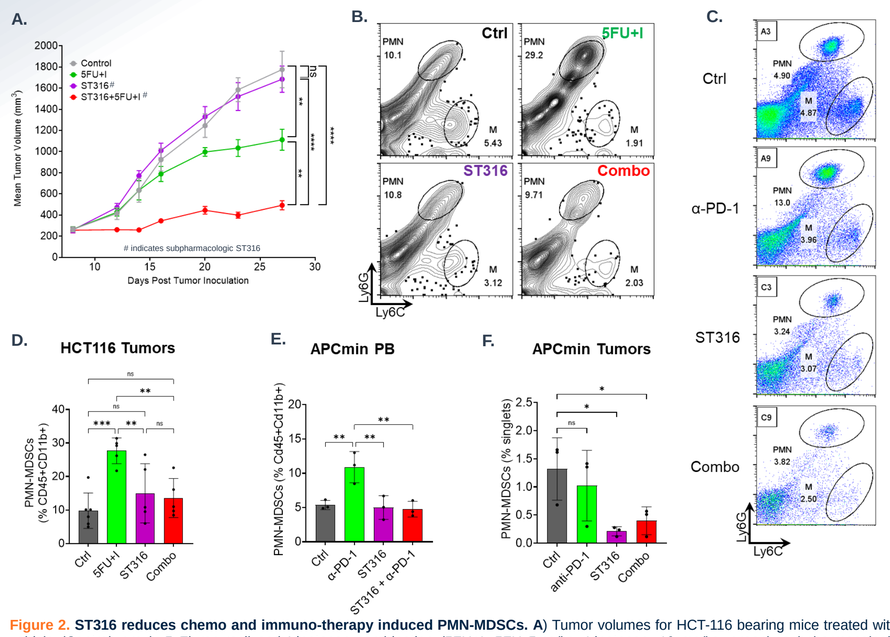

Figure 2. ST316 reduces chemo and immuno-therapy induced PMN-MDSCs. A) Tumor volumes for HCT-116 bearing mice treated with vehicle (Control, grey), 5 Flurururacil and Irinotecan combination (5FU+I; 5FU 5mg/kg; Irinotecan, 10 mg/kg; green), subpharmacologic ST316 (2 mg/kg, 1x/week; violet) and ST316 and 5FU+I combination (red). **B**) Representative flow cytometry plots of $CD11b^+CD45^+$ cells gated for PMN- ($Ly6G^+Ly6C^{int}$) and M-MDSCs ($Ly6G^-Ly6C^+$). Cells were derived from single-cell suspension of HCT116 tumors treated as indicated. **C**) Representative flow cytometry plots for PMN- ($Ly6G^+Ly6C^{int}$) and M-MDSCs ($Ly6G^-Ly6C^+$) gated from Peripheral Blood (PB) of APC^{min} mice treated as indicated (Control; anti-PD-1 (BioXCell #BE0146, clone 29F.1A12; 12.5 mg/kg/wk); subpharmacologic ST316 (2mg/kg 1x/wk); Combination). **D-F**) Bar chart for frequency of D) PMN-MDSCs gated as described in B from HCT116 tumors; **E**) frequency of PMN-MDSCs from PB of APC^{min} mice gated as described in C; and F) frequency of PMN-MDSCs from colon resections of 3-month treated APC^{min} mice. n=6/group (A, B and D) or n=3/group (C, E and F). Statistics, 1-way Anova, ****p<0.001; ***,p<0.001; **p<0.01; *p<0.05; ns, not significant. Error bars represent standard deviations.

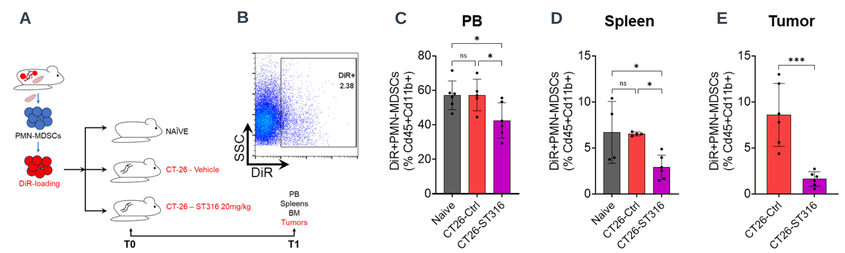

Figure 2. Syngeneic transplanted PMN-MDSCs persist in vivo independently of tumor, colonize haemopoietic sites and are suppressed by ST316 exposure. A) Experimental scheme for DiR-loaded PMN-MDSCs transplant into naïve or CT-26 tumor-bearing BALB/c mice. PMN-MDSCs were sorted from CT-26 tumor bearing donor mice, loaded with DiR (DiIC18(7) (1,1'-Dioctadecyl-3,3,3',3'-Tetramethylindotricarbocyanine Iodide)) and transplanted in syngeneic Naïve or CT-26 tumor-bearing Balb/C mice. Recipient mice were treated with vehicle or 20 mg/kg ST316 for 1 week (2 total doses administered 24 hrs post transplant and 24 hrs prior to harvest). **B**) Representative flow cytometry plot for DiR^+ myeloid cells (gated as $CD11b^+CD45^+$). **C-E)** Bar chart for DiR+ PMN-MDSC (as CD45+CD11b+ fractions) in peripheral blood (**C**), spleen (**D**) and tumors (**E**) of Balb/C mice of the indicated cohorts. Statistics, 1-way Anova, T-test. *p<0.05; ***p<0.001; ns, not significant). Error bars represent standard deviations.

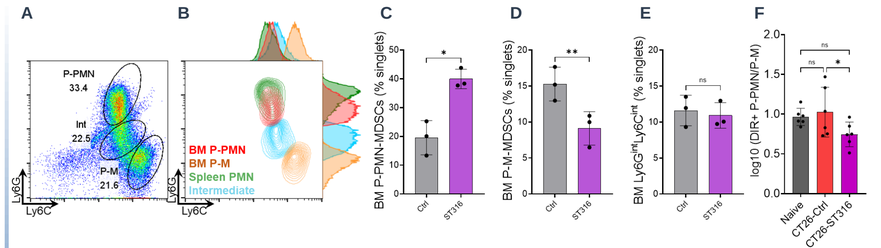

Figure 4. ST316 shifts the ratio between MDSCs precursor populations in bone marrow, suggesting a β-catenin-BCL9 role in PMN-MDSCs generation. A) Representative gating of bone marrow single cell suspension from APC^{min} mice. Gating identifies $Ly6G^{high}Ly6C^{low}$ (precursors PMN-MDSCs, P-PMNs), $Ly6G^{low}Ly6C^{high}$ (precursors M-MDSCs, P-Ms) populations and a $Ly6G^{mid}Ly6C^{mid}$ (Intermediate) population. **B**) Comparison of Ly6G and Ly6C staining intensity for PMN-MDSCs from spleen (Spleen PMN, green), P-PMN and P-M from bone marrow (BM P-PMN, red; BM P-M, brown) and the Intermediate population (cyan) defined in A. **C-E**) Bar graphs of C) P-PMN-MDSCs D) P-M-MDSCs and E) intermediate populations in bone marrow of APC^{min} mice treated with vehicle (Ctrl) or ST316 as described in Figure 3. Statistics, Student t-test.**p<0.01; *p<0.05; ns, not significant, n=3/group. **F**) Ratio of P-PMN to P-M in DiR-PMN-MDSCs transplanted CT26-animals as described in Figure 3. Statistics, Student t-test. *p<0.05; ns, not significant, n=6/group.

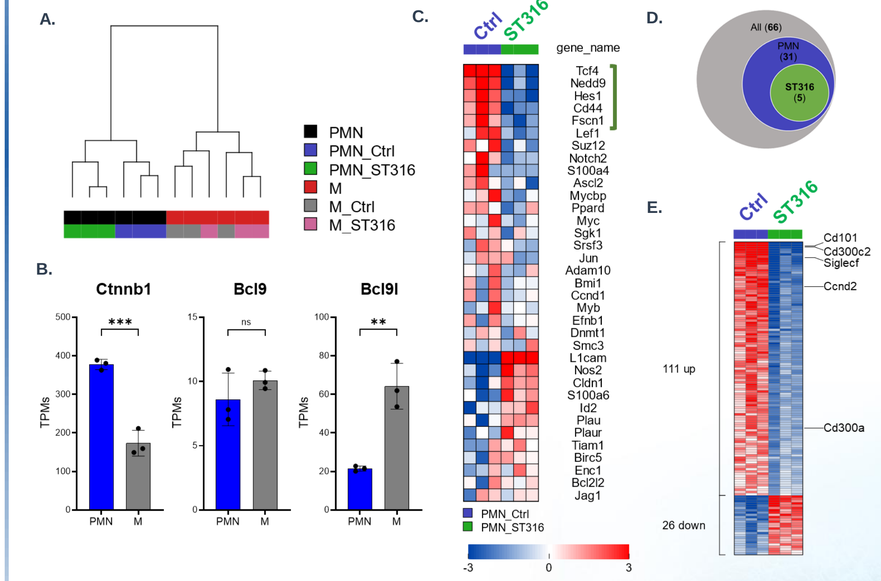

Figure 5. ST316 shifts the transcriptional program of PMN-MDSCs in vivo. A) Unsupervised clustering of splenic PMN- and M-MDSCs transcriptional profiles (n=3 each). Highest level clustering shows PMN- and M-MDSCs are readily separated while ST316 treatment separates PMN- but not M-MDSCs. Spleens were resected from CT-26 bearing mice treated with vehicle (Control) or 20 mg/kg ST316 as in Fig. 3. **B**) β-catenin, Bcl9 and Bcl9l are robustly expressed in MDSCs. **C**) Heat-map showing a subset of β-catenin canonical signature (Herbst et al., 2014) is suppressed by ST316. Out of the 66 genes of the original signature, 33 are expressed in PMN-MDSCs and 5 are significantly (p<0.05) suppressed by ST316 exposures (green bracket). **D)** Venn diagram showing relation between β-catenin targets and ST316 suppression. **E**) Supervised clustering shows 111 targets are suppressed by ST316 in PMN-MDSCs, including several myeloid receptors previously linked to immunosuppressive roles (Sigle-cf, Cd101, Cd300c, Cd300a). Heatmap indicates genes with TPMs greater than 20 in at least two samples, fold change between Control and ST316-treated greater than 2 and a p-value less than 0.05 (BH correction).

Conclusions

1. Chemotherapy and Immunotherapy-driven increases in MDSCs are reverted by ST316 exposure in vivo. ST316 exposure decreases PMN-MDSCs in spleen and tumors in three in vivo CRC models.
2. In vivo tracking reveals that PMN-MDSCs persist in vivo independently of tumor and that ST316-mediated suppression of PMN-MDSCs occurs in both haemopoietic compartments and tumors. In bone marrow, ST316 inverts the ratio between PMN- and M-MDSC precursor populations, suggesting beta-catenin/BCL9 controls an early differentiation step in MDSCs generation.
3. Transcriptional profiling reveals that PMN-MDSCs express robust levels of beta-catenin and Bcl9/9l. ST316 suppresses a subset of canonical Wnt/Beta-catenin targets and receptors previously linked to the immuno-suppressive activity of MDSCs.
4. All together, these data support ST316 combination strategies with immunotherapy and standard-of-care agents and suggest ST316 may act in part by attenuating MDSC immunosuppressive properties.

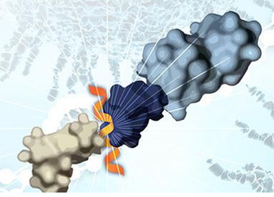

Confidential © 2025 Sapience Therapeutics, Inc.
Contact information: jrotolo@sapiencetherapeutics.com